Impact of Antenna Pattern Modeling Errors on RSSI-based DOA Estimation

Martin Wohler*, Markus Hartmann†, Thorsten Nowak†, Albert Heuberger*
*Fraunhofer Institute for Integrated Circuits (IIS), 91058 Erlangen, Germany
Email: martin.wohler@iis.fraunhofer.de
†Friedrich-Alexander-Universität Erlangen-Nürnberg (FAU), 91058 Erlangen, Germany

***Abstract*—In this paper, we elaborate a reference antenna in terms of direction of arrival (DOA) estimation accuracy to verify its reliability under realistic propagation conditions. Estimation accuracy decreases for the reference antenna due to environmental influences. Our main contribution is modeling such non-anechoic environment in the simulation by considering proximity to earth with surface roughness, antenna cover against climatic influences and height of the stacked-up system over earth in a real-world deployment. We developed a ring extension for the antenna, such environmental influences are minimized and the DOA estimation accuracy is improved again. The overall localization performance of a system with several DOA estimation sensor nodes for different antenna configurations is proven in a simulation environment. The results show an improvement of the localization accuracy for the optimized antenna.**

I. Introduction

Ongoing research in wildlife tracking and behavioral studies requires tracking systems to observe multiple individuals simultaneously. For large areas and mid-sized bats GNSS-based systems have been successfully deployed [1]. For small and lightweight animals these systems are not applicable due to strict weight restrictions. Mid-range observations of hunting behavior require a large number of cost-effective sensor nodes for a sufficient coverage. Furthermore, wildlife tracking systems should provide consistent localization performance in changing real-world environments, e.g. forest. The performance of the overall system depends on the individual parts, the antenna in particular.

The authors of [2] presented a switched beam antenna for direction of arrival (DOA) estimation based on received signal strength (RSS). An optimal radiation pattern for RSS-based DOA estimation has been derived and synthesized in [3] for arbitrary antennas. A prototyped version of the optimal antenna array, the reference design considered in this paper, has been presented in [4].

The proposed prototype provides a nearly optimal pattern realized by a passive beam-forming feed network. The reference antenna showed good performance in field tests, but does not achieve the expected localization accuray, due to the lack of realistic simulation environment. In this paper we investigate the additional influences of the environment and the sensor node setup to the antenna pattern. We minimize the influence of the environment by a ring extension to the antenna and by this improve the localization accuracy.

The paper is organized as follows. Section II covers the influences of real environment on the array behavior, its impact and the array adaption. Section III presents the resulting estimation errors between a not optimized and optimized antenna. Section IV concludes the paper.

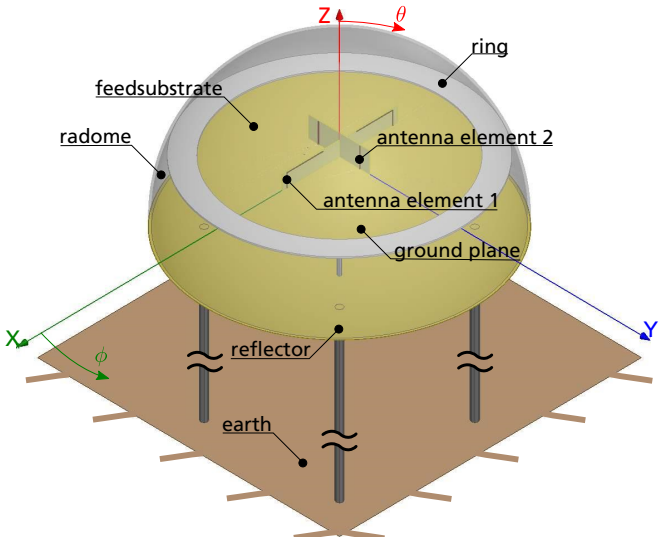

Fig. 1: Stacked-up setup with the antenna in a simplified environment over conductive earth.

II. Antenna in Ideal and Non-Anechoic Environments

As pointed out in [3] and [5] the main factors for field strength-based DOA estimation are the ambiguity of an estimation and the minimum achievable accuracy of an unbiased estimator. This estimator can be described by the Cramer Rao Lower Bound (CRLB) and the geometrical arrangement of the sensor nodes of an localization system. The DOA of an radio signal can be inferred from RSS difference as expressed by:

$$\Delta G(\varphi) = G_{\mathrm{RX},1}(\varphi) - G_{\mathrm{RX},2}(\varphi) \approx \Delta P_{\mathrm{RX}}(\varphi), \qquad (1)$$

where φ is the DOA. $G_{\mathrm{RX},1}$ and $G_{\mathrm{RX},2}$ are the gain functions in dB of the antenna w.r.t. the DOA φ. In an environment without multi-path or low multi-path $\Delta G(\varphi) \approx \Delta P_{\mathrm{RX}}(\varphi)$.

There are two main error sources for the RSS based DOA estimation: multi-path effects, i.e., multiple signals are superimposed and received at the antenna and, modeling errors of the gain pattern $G_{\mathrm{RX},i}$ of the antennas. The antenna is

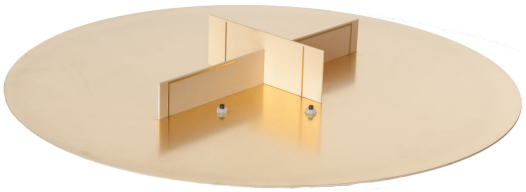

Fig. 2: Photo of the prototype antenna showing the two monopoles for 2.4 GHz and the two folded monopoles for 868 MHz.

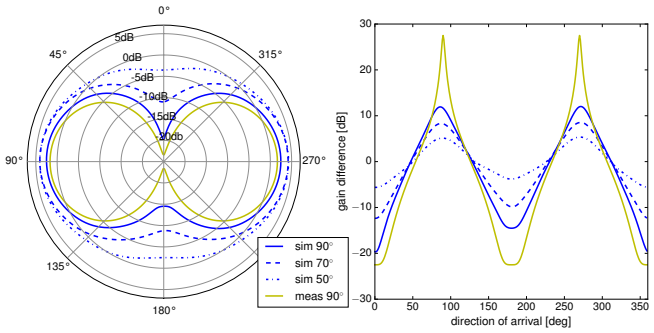

Fig. 3: Gain pattern and gain difference of a measured antenna in anechoic environment compared to the simulated pattern of the stacked-up antenna over earth at different co-elevation plane amplitude patterns ($\vartheta = 50\,°, 70\,°, 90\,°$) at 868 MHz.

sensitive to changes in the surrounding. If this is not modeled correctly or compensated, it leads to DOA estimation errors. Furthermore the antenna is sensitive to the height of operation over ground, i.e., the radiation characteristic does not resemble the assumed ideal beam.

The designed antenna array [4], presented in Fig. 2, shows good agreement between simulation and measured radiation characteristic on the entire upper hemisphere in an anechoic environment. Assuming a spherical coordinate system where φ is the azimuth angle and ϑ is the co-elevation angle as illustrated in Fig. 1. As a reference the horizontal radiation characteristics of the measured antenna with their associated gain functions are shown in Fig. 3. However, to take into account the realistic test-setup, the system (cf. Fig. 1) is stacked-up in a certain distance over ground. The field strength is a function of φ and ϑ. ϑ is chosen as $50\,°$, $70\,°$ and $90\,°$. It can be seen in Fig. 3 that also the gain difference as a function of φ varies with varying ϑ: $\Delta G_{\mathrm{RX}}(\varphi) = f(\vartheta)$. Furthermore for $\vartheta = 90\,°$ the ideal $\Delta G(\varphi)$ ('meas') exceeds the gain difference when the antenna is mounted over earth ('sim'). Within this setup and a real-world environment the localization properties of the DOA change. An error in modeling of the antenna gain pattern $G_{\mathrm{RX},1}$ and $G_{\mathrm{RX},2}$ directly decreases the DOA estimation accuracy (cf. Fig. 3) as resulting in smaller field strength differences.

A. Antenna Properties

As expressed in (1), the higher the gain differences between the two pattern ($G_{RX,1}, G_{RX,2}$), the steeper is the resulting gain difference function and thus, the more accurate is the estimation of the DOA φ [4]. Simulations reveal for the stacked-up setup (Fig. 1) that the gain difference function $\Delta G(\varphi)$ reduces towards zero for low co-elevations. To increase the difference, the antenna properties have to be altered. Therefore the influences of the setup to the antenna is in the following derived. Conveniently, we start with the general hertzian half-wave dipole. It has a rotational symmetrical radiation characteristic, e.g. the radiation characteristic of a single / vertical dipole, aligned in z-axis, reads:

$$C_{\mathrm{e}}(\vartheta) = \frac{\cos\left(\frac{\pi}{2}\cos\vartheta\right)}{\sin\vartheta}. \tag{2}$$

The array factor (C_{gr}) is a function of the positions of multiple antenna elements, which denote the radiation characteristic originating from an array of those elements [6]. This group factor describes a complex weighted superposition of N antenna elements given by:

$$C_{\mathrm{gr}}(\varphi,\vartheta) = \sum_{i=0}^{N-1} w_i e^{-jk_0 r_i}, \tag{3}$$

where w_i defines the magnitude and phase of the i-th element feeding and, k_0 is the wave vector of the incident wave. r_i is the distance between the i-th element position and the point of observation in the far field w.r.t the DOA. The characteristic of the entire array C_{array}, is obtained by:

$$C_{\mathrm{array}} = C_{\mathrm{e}} \cdot C_{gr}. \tag{4}$$

The reference antenna [4], shown in Fig. 2, consists of two vertically aligned monopoles. Compared to this the sub-array at 868 MHz consists of two folded monopoles. The elements length is close to $0.25\lambda_0$, where λ_0 is the wavelength in free space.

The fields of both sub-arrays above the ground-plane can be deduced from the resulting fields of the single monopole, (2) and its image (3) and (4). Those characterize a single antenna element ($N = 2$). Due to the vertical alignment of the monopole over ground the radiation characteristic with equal weighted elements and in-phase feeding is defined by:

$$C_{\mathrm{array}} = \frac{\cos\left(\frac{\pi}{2}\cos\vartheta\right)}{\sin\vartheta} \cdot \left|\cos\left(k_0 h_e \cos\vartheta\right)\right|, \tag{5}$$

where h_e the height over the ideal conducting ground. The height of an antenna element over ground changes the radiation characteristic [7]. The characteristic equals the radiation characteristic of a longer monopole. The element characteristic of the second monopole changes as well, i.e. radiation characteristic pattern of the two monopoles at $0.5\lambda_0$ distance alters the gain difference function, which introduces an additional error in the DOA estimation. Hence, to counteract the influence of the height have to be minimized. By changing from horizon to lower co-elevations the co-elevation plane amplitude pattern becomes rounder and the gain pattern modeling error

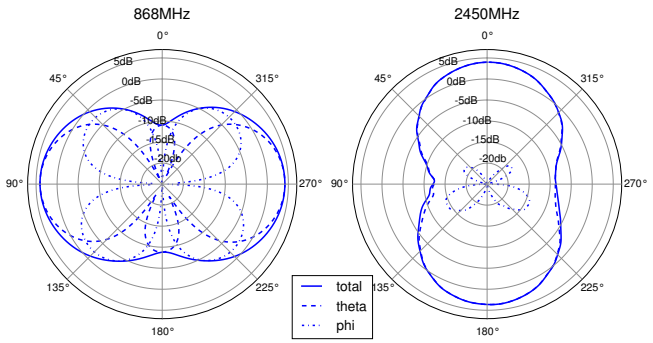

Fig. 4: Co-elevation plane amplitude patterns at $\vartheta = 70\,^\circ$ for $G_{\mathrm{RX},1}(\vartheta)$, $G_{\mathrm{RX},1}(\varphi)$ and $G_{\mathrm{RX},1,\mathrm{Total}}(\varphi,\vartheta)$ of the antenna for the stacked-up setup at both frequencies: 868 MHz and 2450 MHz.

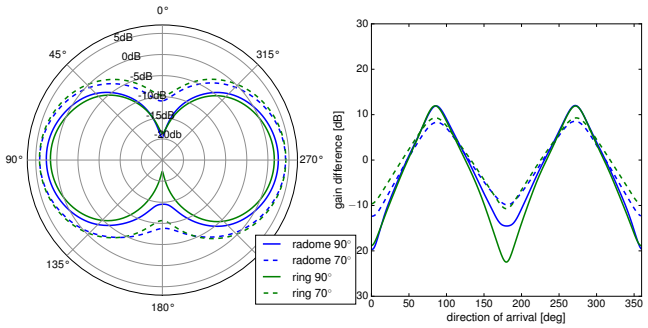

Fig. 5: Comparison of the simulated co-elevation plane amplitude patterns at $\vartheta = 70\,^\circ$ and $\vartheta = 90\,^\circ$ for $G_{\mathrm{RX},1,\mathrm{Total}}(\varphi,\vartheta)$ of the antenna in the stacked-up setup with and without ring at 868 MHz.

increases. This effect is shown in Fig. 3 with flattening of the gain difference for lower co-elevations ($\vartheta = 50°$).

B. Polarization and Ground Effects

For an implemented antenna the ground-plane is restricted to a limited size due to economical and practical reasons. Following [8] in a real environment an electrically small ground plane reduces the performance of the array in several manners. It reduces the element directivity near horizon as shown in Fig. 3 by comparing the maximum gain between $\vartheta = 50°$ and $\vartheta = 90°$. Furthermore it decreases the element radiation efficiency caused by earth losses. The earth also acts as a reflector for an antenna. The reflective properties of the earth are determined by the dielectric constant (ε_r) and the conductivity (σ). Since the conductivity of earth is limited, a part of the radiated energy of the antenna is also absorbed [8].

For wildlife tracking the reference antenna array is located in the forest, e.g. rain forest or dry wood forest. We define the environment as medium dry earth ($\varepsilon_r = 15.0\,, \sigma = 0.001\,\mathrm{S/m}$). Furthermore, to protect the antenna against rain, a housing is required. For a rectangular housing there is a negligible difference in antenna performance in comparison without housing. However, tests reveal that already 100 ml water close to the antenna influencing the antenna characteristic heavily. So water standing on the top of a rectangular housing influences the antenna. Hence, a spherical radome is chosen, which influence the radiation characteristic slightly but is unaffected in case of rain.

Relating to the reference array, the orientation of the antennas, either horizontal or vertical, relative to the ground is crucial. In a vertically aligned antenna the current distribution of the original element and its reflection image are in-phase. For horizontal oriented antennas the current of the mirror image is out-of-phase. The one sub-array ($f_H = 2.45\,\mathrm{GHz}$) consists of vertical-polarized monopoles with a finite ground-plane. However the far-field radiated power density near horizon is determined by the current distribution on the monopoles and not the ground plane current [8]. It can be seen that $G_{\mathrm{RX},1,\mathrm{Total}}(\varphi,\vartheta)$ at $f_H = 2.45\,\mathrm{GHz}$ in Fig. 4 is mainly shaped by $G_{\mathrm{RX},1}(\vartheta)$. Due to the previously outlined impact of the earth at the stacked-up setup the folded monopoles ($f_L = 868\,\mathrm{MHz}$) add up a horizontal field component. This result in a transverse component interfered by earth. To illustrate this effect the gain components are presented for the co-elevation plane amplitude pattern for $\vartheta = 70°$, the horizontal component ($G_{\mathrm{RX},1}(\varphi)$) adds to the $G_{\mathrm{RX},1}(\vartheta)$, resulting in rounder $G_{\mathrm{RX},1,\mathrm{Total}}(\varphi,\vartheta)$. This effect increase with lower co-elevation angles (cf. Fig. 3).

C. Impact to the Prototype

The objective is to minimize the influence of the environment to the antenna to obtain the eight-like radiation characteristic. Therefore, the ground plane diameter could be expanded with ease, but leads to minimal improvements, only. A prospective approach is found with the choke ring. Briefly said, a choke ring antenna consists of a number of conductive concentric cylinders around a central antenna. The idea is adapted by introducing several rings on top of the homogeneous finite ground plane of the central antenna. A single-depth ring with 2 mm height attenuate the non-desired incoming waves from high co-elevation angles, e.g. by earth. The ground plane extension is already illustrated in Fig. 1. Their results are presented in Fig. 5. The ring with its additional discontinuity in the ground-plane improves the decoupling between earth and antenna. To sum up, this design realizes the desired gain difference function.

III. Localization Performance

Obviously an error in modeling the gain pattern, as shown in Section II will also influence the localization performance significantly. In a simulation environment the influence of the modeling error of the antenna gain pattern is demonstrated. The simulation environment considers path loss, fading and thermal noise effects. A trajectory in a 2D plane is simulated. The measurement values are generated with respect to the position of the sensor nodes and mobile target. The measurement

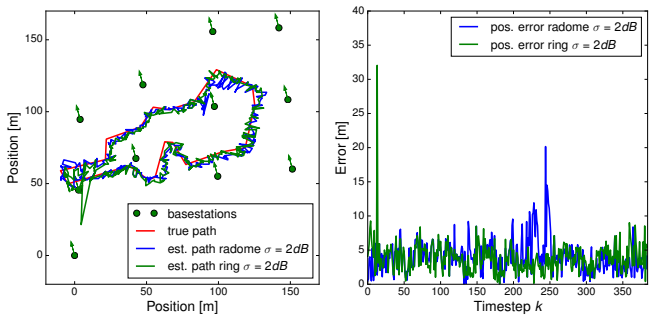

Fig. 6: The left plot shows the sensor node arrangement, true path and localized path. The right plot shows the localization error for every movement step.

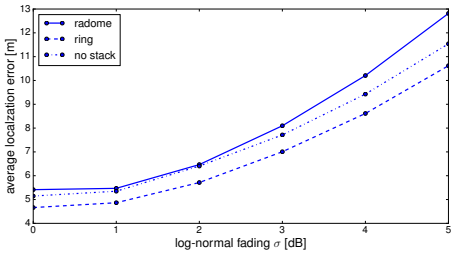

Fig. 7: The average localization error w.r.t. the parameter σ of the log-normal fading.

values are manipulated by fading and used in a localization algorithm for a position estimation [9]. For the simulation the measurement values are given by

$$\tilde{P}_{RX,i} = P_{RX,i} + v_i \quad \text{with} \quad v_i \sim \mathcal{N}(\mu, \sigma), \tag{6}$$

where $P_{RX,i}$ is the true RSS value for antenna i in dB and $\tilde{P}_{RX,i}$ is the simulated value, which represents a measurement, also in dB. The added fading v_i is normal distributed in the logarithmic scale, where $\mu = 0$ [10], [11]. The estimated trajectory is compared to the true simulated trajectory. In Fig. 6 the setup of the sensor nodes and the true path are shown. Furthermore the localized path by a fading $\sigma = 2\,\mathrm{dB}$ is presented. The right subplot illustrates the localization error over distance, shown per time-step k. It can be seen that different kinds of antenna configurations result in different localization errors.

For a simplified analysis the average position localization error for the full path is calculated. In Fig. 7 the numbers for different levels of fading are presented. The influence of the earth and the radome are also considered in Fig. 7. Thereby the localization error increases from the reference design in the free space ('no stack', Fig. 2) by implementing the configuration over earth and with radome ('radome', Fig. 1). The improved antenna version with the additional ring, minimizes the effect of the earth and improves the localization performance significant in the full simulation range of fading from $0\,\mathrm{dB} \leqslant \sigma \leqslant 5\,\mathrm{dB}$ as shown in Fig. 7.

IV. Conclusion

Under realistic propagation conditions the accuracy of the DOA estimation decreases with the reference antenna. By modeling the entire stacked-up system with radome, antenna and earth in the simulation, the interaction reveal the necessity to add an expanded ground-plane to achieve a similar localization performance as in the ideal environment. It is shown by the estimated and true simulated trajectory that the localization errors decrease within the non-anechoic environment when ring is added above the ground-plane to the reference antenna. The system performance has been verified by applying a simulation in 2D plane for a trajectory with different fading levels. The minimized interaction yield in an improved localization performance over the full simulation range. Yet, the antenna is resistant against environmental circumstances and a effective solution for low-cost sensor networks.

Acknowledgment

This work is supported by German Science Foundation DFG under Grant FOR 1508, Research Unit BATS. Furthermore, the authors are grateful to their colleague Mario Schühler for his helpful comments.

References

[1] Noam Cvikel, Katya Egert Berg, Eran Levin, Edward Hurme, Ivailo Borissov, Arjan Boonman, Eran Amichai, and Yossi Yovel. Bats aggregate to improve prey search but might be impaired when their density becomes too high. *Current Biology*, 25(2):206–211, 2015.

[2] G. Giorgetti, S. Maddio, A. Cidronali, S. K S Gupta, and G. Manes. Switched beam antenna design principles for angle of arrival estimation. In *Wireless Technology Conference, 2009. EuWIT 2009. European*, pages 5–8, Sept 2009.

[3] Markus Hartmann, Oliver Pfadenhauer, Lucila Patino-Studencka, Hans-Martin Troeger, Albert Heuberger, and Joern Thielecke. Antenna pattern optimization for a rssi-based direction of arrival localization system. In *Proceedings of the ION 2015 Pacific PNT Meeting*, pages pp. 429–433, 2015.

[4] Markus Hartmann, Martin Wohler, Mario Schuehler, Lars Weisgerber, Jörn Thielecke, and Albert Heuberger. A dual frequency antenna for rssi-based doa estimation - from theory to prototype. In *Proceedings of the Days of Diffraction 2016*, 2016.

[5] Thorsten Nowak, Markus Hartmann, Thomas Lindner, and Jörn Thielecke. Optimal network topology for a locating system using rssi-based direction finding. In *IPIN 2015 Sixth International Conference on Indoor Positioning and Indoor Navigation (IPIN 2015)*, Banff, Canada, October 2015.

[6] Constantine A Balanis. *Antenna theory and design*. John Wiley & Sons, Inc, 1997.

[7] K.W. Kark. *Antennen und Strahlungsfelder: Elektromagnetische Wellen auf Leitungen, im Freiraum und ihre Abstrahlung*. Springer Fachmedien Wiesbaden, 2014.

[8] M.M. Weiner. *Monopole Antennas*. CRC Press, 2003.

[9] Markus Hartmann, Thorsten Nowak, Oliver Pfadenhauer, Joern Thielecke, and Albert Heuberger. A grid-based filter for tracking bats applying field strength measurements. In *Proceedings of the 2016 IEEE/IFIP Wireless On-demand Network systems and Services Conference*, pages 184–191, 2016.

[10] D.C. Cox, R.R. Murray, and A.W. Norris. 800-MHz attenuation measured in and around suburban houses. *AT&T Bell Laboratories Technical Journal*, 63(6):921–954, 1984.

[11] John S. Seybold. *Introduction to RF propagation*. John Wiley & Sons, 2005.